The University of
Nottingham

UNITED KINGDOM · CHINA · MALAYSIA

Rouse, James Paul and Hyde, Christopher J. and Sun, Wei and Hyde, T.H. (2013) Comparison of several optimisation strategies for the determination of material constants in the Chaboche visco-plasticity model. Journal of Strain Analysis for Engineering Design, 48 (6). pp. 347-363. ISSN 2041-3130

Access from the University of Nottingham repository:

http://eprints.nottingham.ac.uk/46517/1/Comparison%20Rouse%20-%20JSA%20Manuscript%20-%20ePrints.pdf

Comparison of Several Optimisation Strategies for the Determination of Material Constants in the Chaboche Visco-Plasticity Model

J. P. Rouse[*], C. J. Hyde, W. Sun, T. H. Hyde

Department of Mechanical, Materials and Manufacturing Engineering
University of Nottingham, University Park
Nottingham, NG7 2RD, UK

Abstract

Determining representative material constants sets for models that can accurately predict the complex plasticity and creep behaviour of components undergoing cyclic loading is of great interest to many industries. The Chaboche unified visco-plasticity model is an example of a model which, with the correct modifications, shows much promise for this particular application[1]. Methods to approximate material constant values in the Chaboche model have been well established[2–4]; however the need for optimisation of these parameters is vital due to assumptions made in the initial estimation process[5,6]. Optimisation of a material constant set is conducted by fitting the predicted response to the experimental results of cyclic tests. It is expected that any experimental data set (found using the same values of test parameters such as temperature; the dependency of which is not accounted for in

[*]Corresponding Author James Rouse, Department of Mechanical, Materials and Manufacturing Engineering, University of Nottingham, University Park, Nottingham, NG7 2RD, UK. Email: `eaxjr@nottingham.ac.uk` Tel: +44 (0) 115 84 67683

the original Chaboche model) should yield a single set of optimised material parameters for a given material. In practice this may not be the case. Experimental test programs usually include multiple loading waveforms; therefore it is often possible to optimise for separate, different sets of material constants for the same material operating under comparable conditions. Several optimisation strategies that utilise multiple sets of experimental data to form the objective functions in optimisation programs have been applied and critiqued. A procedure that evaluates objective functions derived from the multiple experimental data types simultaneously (i.e. in the same optimisation iteration) was found to give the most consistently high quality fitting. In the present work, this is demonstrated using cyclic experimental data for a P91 steel at 600°C. Similar strategies may be applied to many constitutive laws that require some form of optimisation to determine material constant values[7].

1 Introduction

During normal operation, some components (such as turbine discs or steam piping) will almost inevitably experience periodic fluctuations in loading. This is particularly true in the cases of the power plant components and aero engines, where not only mechanical loads but also operating temperatures will vary. Such behaviour causes complex interactions between creep and hardening effects due to the accumulation of plastic strain. Material models such as the Chaboche model can represent this behaviour through the use of several internal variables. Through this model, both isotropic hardening (where a yield surfaces size alters however the relative position remains constant[8], see fig. 1 (a)) and kinematic hardening (where a yield surface remains a constant size but alters in its orientation[8], see fig. 1 (b)), as well as creep behaviour, can be represented. In laboratory testing programs conducted at the University of Nottingham, isothermal strain controlled tests, using an Instron 8862 thermo-mechanical fatigue (TMF) machine (utilising radio frequency induction heating) were completed using two main types of loading wave form. In experiments performed on a P91 steel at 600°C(presented later within this paper as an example case for the optimisation procedures), a saw tooth loading profile has been applied. Loads uniformly oscillated between $\pm 0.5\%$ strain (with a fixed strain rate of 0.1%\s, see fig. 2 (a)). This is considered to be the simplest form of loading in this testing program due to the greatly reduced dependence on creep mechanisms. Initial conditions for optimisation procedures are often derived from these results due to the dominant hardening effects observed. Additionally, relaxation or dwell testing has been completed using the same strain limits and rates as applied as in the saw tooth loading experiments. A 2 minute hold period is introduced at the end of each tensile loading region (see fig. 2 (b)). This gives rise to a period of creep dominant behaviour, acting to relax the stresses in the specimen. This more complex behaviour can be used to demonstrate the wide applicability of the Chaboche model and to estimate the creep behaviour for a material. Typical experimental stress responses for the saw tooth and relaxation loading profiles can be seen in fig. 2 (c) and (d), respectively.
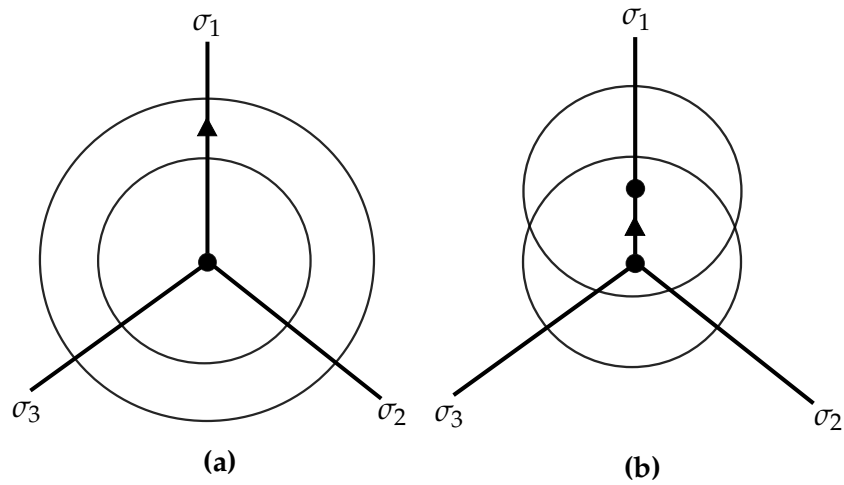
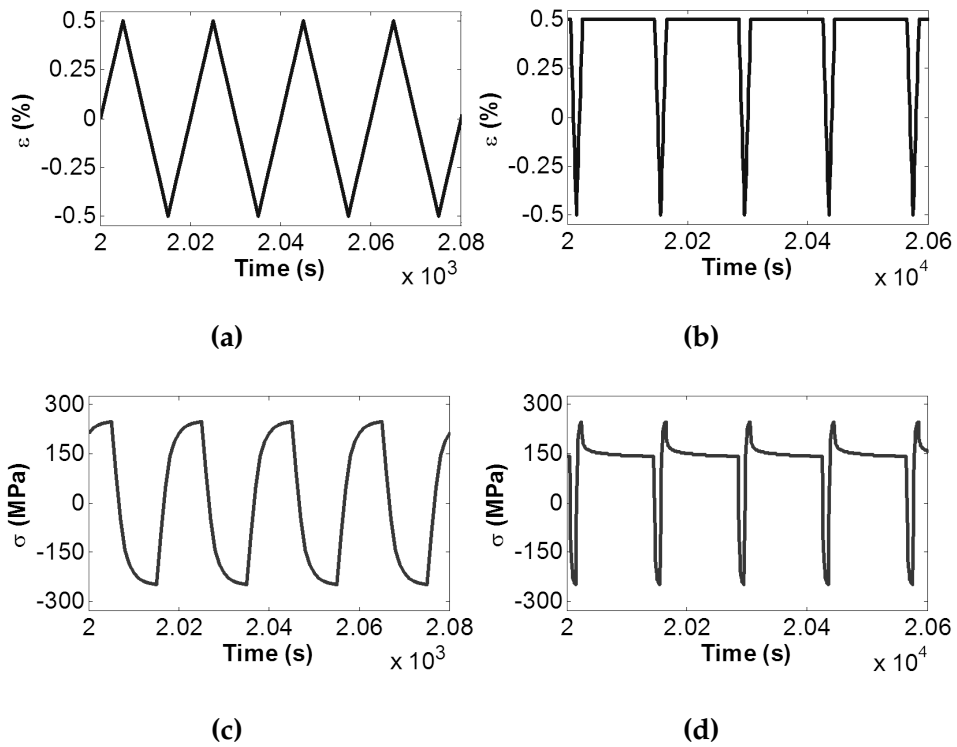**Figure 1:** *Representation of (a) isotropic hardening and (b) kinematic hardening*

Figure 2: *Example of typical (a) saw tooth strain loading profile, (b) relaxation strain loading profile, (c) stress response due to saw tooth loading profile and (d) stress response due to relaxation loading profile (shown for a P91 steel at 600°C).*

2   Mathematical Representations of Visco-Plasticity

2.1   The Chaboche Unified Visco-Plasticity Model

The Chaboche model decomposes total strain into elastic and plastic components, allowing for the interpretation of both kinematic and isotropic hardening through the use of appropriate internal variables. The uniaxial form of the Chaboche model is applied to several optimisation methodologies in this paper and for clarity is described here. In the Chaboche model a single yield function is defined by eq. (1)[9]. Note that the quantities σ and k represent the total stress and a temperature dependent quantity related to the initial cyclic yield surface size[9], respectively. The constant k should not be confused with the tensile yield stress of a material. In strain controlled experimental results, k is usually taken to be the stress at which in-elastic behaviour is first observed in the first full tensile loading region of the first cycle. While initial values of k may be similar to the tensile yield stress, optimised values have been commonly found to be significantly less.

$$f = |\sigma - \chi| - R - k \leqq 0 \tag{1}$$

Only elastic behaviour will occur when the value of this function is less than or equal to 0. The back stress (χ) designates the centre of a yield surface and the drag stress (R) denotes the variation of its size (note this can either act to increase or decrease the size of the yield surface)[9]. Through the use of these quantities, kinematic and isotropic hardening may be represented, respectively. The term $|\sigma - \chi|$ allows for the interpretation of the absolute distance between the loading point and the centre of the yield surface in stress space. To provide a better approximation of the kinematic effects, back stress can be decomposed into several components[1,9] (note in the present study, a two back stress component model was used[5]). An Armstrong and Frederick type kinematic hardening law is used to define the increment for each back stress component, taking the form of eq. (2)[3].

$$d\chi_i = C_i(a_i d\varepsilon^p - \chi_i dp) \tag{2}$$

where a_i and C_i are both material constants (a_i defines the stationary

value of the back stress and C_i dictates how quickly this value is achieved with the increase in plastic strain[3,4]). Additional back stress components can aid in the description of non-linear kinematic hardening behaviour. Components will be dominant in certain hardening regions and recessive in others. The use of multiple back stress components is of particular importance when describing non-linear kinematic behaviour that cannot be adequately represented by a single Armstrong-Frederick expression. Since the present work attempts to identify a preferred optimisation methodology, two back stress components have been adopted with the knowledge that the models ability to predict experimental data may be improved by increasing the number of back stress components. The accumulated plastic strain (p), on which most of the internal variables are dependent, is a monotonic increasing quantity and is the summation of the modulus of the plastic component of total strain (ε_p), or described mathematically in eq. (3)[5] (note that a dot denotes a rate quantity).

$$\dot{p} = \Sigma|\dot{\varepsilon}^p| \tag{3}$$

By decomposing the back stress into multiple components, transient and long term behaviour may be accounted for[2], here with a_1 and C_1 dictating the evolution of χ_1 (which describes initial kinematic non-linearity) and a_2 and C_2 dictating the evolution of χ_2 (describing asymptotic, stabalised behaviour), see fig. 3. The total back stress (χ) is given as a summation of these components; therefore for N components of back stress, the total back stress (χ) is given by eq. (4).

$$\chi = \sum_{i=1}^{N=2} \chi_i \tag{4}$$

The effects of isotropic hardening are represented by the scalar drag stress (R). As such, R will alter only the size of the yield surface, see eq. (5).[9,10]. Note that with the drag stress equation in this form, only primary behaviour (either hardening or softening) can be represented (see fig. 4). The drag stress will undergo some initial monotonic increase or reduction before reaching a stabilised asymptotic value[3–5] (see fig. 4). This

saturated value is signified by Q, with the rate at which the stabilised value is reached being determined by the material constant b, see eq. (5)[5].

$$R = Q(1 - \exp^{-bp})$$ (5)

While saturated behaviour may be physically realistic for a period of time for some materials, for a P91 steel, which is a key high temperature material for power plants, secondary linear softening behaviour is exhibited. This causes a constant gradient secondary section in the stress range versus cycle number curve (fig. 9 shows typical experimental softening stress range curves for a P91 steel), which is not considered in the original model. Ultimately, all materials will soften in the vicinity of failure[8]. Secondary linear effects can be represented through the addition of a linear term (eq. (6)) in the isotropic hardening law (eq. (5)), utilising an extra material constant (here designated H)[11], preventing the saturation of the drag stress. The signs of the saturation constant Q and the secondary hardening rate constant H can be positive or negative, depending on whether hardening or softening behaviour is observed, respectively. Indeed, combinations of positive Q values and negative H values can be implemented for materials that primarily harden but soften in the secondary region (or vice-versa). In this way, combined hardening and softening behaviour is accounted for.

$$R = Q(1 - \exp^{-bp}) + Hp$$ (6)

Creep effects will be present when time or strain rate have an influence on inelastic behaviour[9]. Time dependent creep behaviour can be introduced through the definition of a viscous stress (σ_v), forming a component of total stress, summarised by eq. (7)[3,4], where the scalar components of stress act to increase or decrease the size of the yield surface around its centre (defined by the quantity χ):

$$\sigma = \chi + (R + k + \sigma_v)sgn(\sigma - \chi)$$ (7)

where the function $sgn(x)$ is specified by eq. (8).

$$sgn(x) = \begin{cases} 1 & \text{if } x > 0 \\ 0 & \text{if } x = 0 \\ -1 & \text{if } x < 0 \end{cases} \tag{8}$$

The viscous stress here is assumed to take the form of a power law[9], such as eq. (9).

$$\sigma_v = Z\dot{p}^{1/n} \tag{9}$$

where Z and n are viscous material coefficients. Recalling the definition of the flow rule, paying particular attention to the condition of normality (applicable for the study of metals[12]), and applying the definitions of the yield surface and normal direction[1,9], an expression for the uniaxial plastic strain increment (eq. (10)) can be derived. Note that, as this is the uniaxial form, σ and χ are both scalar quantities (in the multiaxial form they are tensors). Note that the definition of the brackets used in eq. (10) is given in eq. (11).

$$d\varepsilon^p = \left\langle \frac{|\sigma - \chi| - R - k}{Z} \right\rangle^n sgn(\sigma - \chi)dt \tag{10}$$

$$\langle x \rangle = \begin{cases} x & \text{if } x \geq 0 \\ 0 & \text{if } x < 0 \end{cases} \tag{11}$$
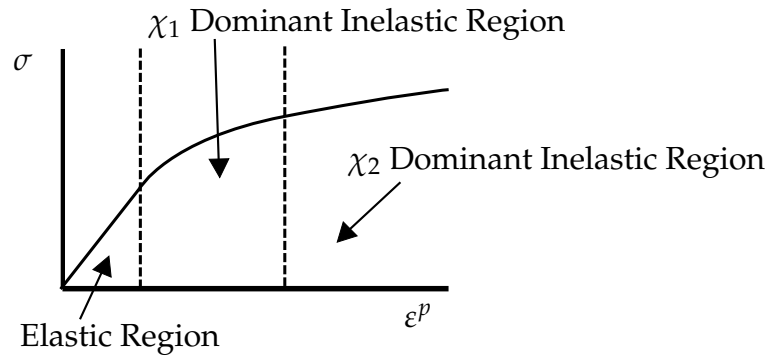

Figure 3: *Evolution of back stress in stress strain space and illustration of dominant components.*
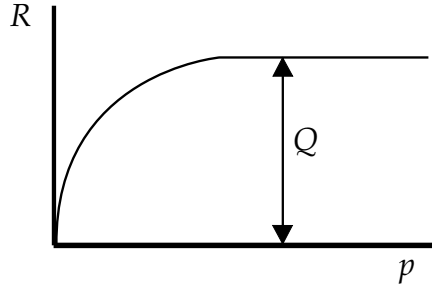
Figure 4: *Evolution of drag stress in the original Chaboche model (shown for a material undergoing primary hardening).*

2.2 Alternative Material Models

The Chaboche model is not the only option available for the representation of hardening behaviour. For completeness, a brief overview of alternatives will be given here. Typically, these involve the definition of a yield function (f) and the implementation of the small strain hypothesis, whereby total strain (ε) may be decomposed into elastic (ε_e) and plastic (ε_p) components, as shown in eq. (12).

$$\varepsilon = \varepsilon_e + \varepsilon_p \tag{12}$$

In the short term, kinematic work hardening is the more realistic as it accounts for the Baushinger effect and anisotropy due to plastic deformation[13], however its predictive capability can be compromised if more complex loading histories are considered. Prager suggested eq. (13) for the yield surface translation increment $d\alpha_{ij}$[14].

$$d\alpha_{ij} = Cd\varepsilon_{ij}^p \tag{13}$$

The translation increment is dependent on a material constant C, known as the hardening modulus[13], and the increment of plastic strain ($d\varepsilon_{ij}^p$). The yield surface is taken to translate in the direction on the outward unit normal to the yield surface[14]. This direction is distinctly different to the modification proposed by Ziegler, where the yield surface translation increment is dependent on a multiplier ($d\mu$) that is greater than zero and

will move in the direction of a vector between the centre of the yield surface and the stress point[15], see eq. (14).

$$d\alpha_{ij} = d\mu \left(\sigma_{ij} - \alpha_{ij} \right) \tag{14}$$

Pragers model exhibits linearity in stress strain predictive behaviour, and as such encounters problems when used in conjunction with complex loading patterns, particularly when loadings and subsequent unloadings are applied along different stress paths[1]. A lone kinematic hardening behaviour law will predict, in the case of alternating plastic strain, that steady state behaviour will be realised after a single loading cycle[13], (this is at odds with experimentally observed results).

As a solution to this difficulty, Mroz proposed the concept of "field of work hardening moduli"[13]. Rather than a single effective plastic modulus being assumed, the hardening curve is approximated by several linear sections, each relating to a different plastic modulus. Mathematically, this can be represented in stress space by a collection of circles, each defined by a yield function.

For an initially isotropic material, these surfaces are similar and share the same origin[13]. Surfaces are assumed to be unable to intersect and instead, if contact is made, multiple surfaces will consecutively connect with subsequent surfaces and move as one[13]. As the stress point traverses stress space, it will come into contact with the first yield surface, if the elastic domain limit is exceeded. With the onset of yielding, an alternative "plastic" modulus is calculated. This active surface will translate along the vector connecting stress point considered and the corresponding stress point on the following surface[1]. By use of this condition, the outward normal on each surface will coincide with one another when surfaces come into contact.

The Mroz model has several advantages over the more simplistic models, such as its ability to predicted the non-linear stress strain loops in material response and describe the Bauschinger effect[8]. Under asymmetric loading conditions however, no ratchetting (where, in a stress limit test, the mean strain increases with cycles, which may reach an approximately steady value or continue to increase leading to failure[8]) is predicted due to

a lack of isotropic hardening in cyclic stable conditions[1]. A clear practical drawback in terms of application however of the Mroz model is that, to describe the response of a material with sufficient accuracy, large numbers of surfaces may be required, each surface requiring the storage of a tensor (most commonly of around six components, representing the centre of each surface) and scalar variable (indicating a surfaces size)[1].

Potential solutions to this problem were proposed by envisaging a two surface model, consisting of a yielding surface and a bounding, limit surface[1]. An example of such a formulation is the Dafalias-Popov model[16]. The plastic modulus (K) becomes a function ($\hat{K}$, eq. (15)) of two distances in stress space (δ, δ_{in})[16].

$$K = \hat{K}\left(\delta, \delta_{in}\right) \tag{15}$$

Where δ represents the stress distance between the stress point and the limit[16], and is quantified by comparing the stress point on the yield surface to the corresponding stress point on a bounding surface, shown in eq. (16) (note that barred parameters relate to the bounding surface).

$$\delta = \left[\left(\bar{\sigma}_{ij} - \sigma_{ij}\right) - \left(\bar{\sigma}_{ij} - \sigma_{ij}\right)\right]^{1/2} \tag{16}$$

The use of this distance allows a continuously variable plastic modulus[16]. The initial value of this distance (i.e. the stress distance at the end of elastic deformation), δ_{in}, will change at each reversal but is constant during plastic flow[16]. Effectively, the yield surface takes the role of the active surface in the Mroz model, while the bounding surface represents the subsequent surface. Both the yield surface and bounding surface will undergo kinematic and isotropic behaviour. While hardening behaviour can be easily described by the Dafalias-Popov model, the inclusion of viscous behaviour is still not accounted for. This is not only relevant in hold periods where creep will be a dominant deformation mechanism, but also in hardening loops where relaxation will occur.

3 Optimisation Procedure

3.1 Requirement

The need for optimisation procedures in determining material constant values that will result in good fits to experimental data is vital when implementing the Chaboche model. The procedure for determining initial estimates of the material constants is detailed elsewhere[2,3,5,6] and will not be repeated here. The requirement for optimisation stems from the assumptions made (e.g. by Tong et al.[3]) when estimating initial values for the material constants, namely:

- Initially, all hardening is assumed to be isotropic (the kinematic state variables are assumed to be zero), allowing for the saturation value Q to be determined (see fig. 4). The remaining isotropic hardening parameter (b) is found by considering the variation of $\Delta\sigma/2$ with the accumulated plastic strain (p) before saturation.

- When estimating kinematic hardening constants, it is assumed (for the integration of the related differential equations, see Tong et al.[3]) that the viscous stress (σ_v) remains constant (i.e. it is not a function of time), for simplification.

- It is assumed that the contribution of χ_1 is negligible in the latter stages of kinematic hardening (see fig. 3). The effects of χ_2 may therefore be isolated and applied only to the later stages of hardening.

- Commonly, initial estimates of the visco-plastic material constants (Z and n) are approximated by trial and error or taken from literature to provide a reasonable fit to the stress relaxation regions[5].

3.2 General Overview and Implementation

In the present work, optimisation iterations are evaluated against each other through the least squares method. In total, three general objective function forms have been developed to define the fitting quality of a predicted stress-time profile to experimental data in the case of strain controlled isothermal

cyclic testing. By using multiple objective functions, preference can be given to areas of great interest in the stress-time profile (such as peak stress values) while overall fitting is still accounted for elsewhere.

General stress fitting is accounted for in the first objective function (eq. (17)).

$$F_1(x) = \sum_{i=1}^{M_1} \left(\sigma(x)_i^{pre} - \sigma_i^{exp} \right)^2 \tag{17}$$

where each experimental stress value (σ_i^{exp}) is compared with the corresponding predicted stress value ($\sigma(x)_i^{pre}$). The quantity M_1 is the total number of experimental points considered in the optimisation. It is of particular importance that the optimisation takes account of the hardening/softening behaviour of the material, as this represents the evolution of the yield surface and stress with cyclic loading. An objective function is therefore created based on the comparison of experimental and predicted stress range values. These can be found by taking the difference between the peak stresses (found at the end of a tensile loading region) and the minimum stresses (realised at the end of a compressive loading region) and dividing by two for each cycle in turn, for both predicted ($\Delta \sigma(x)_i^{pre}/2$) and experimental ($\Delta \sigma_i^{exp}/2$) results (see eq. (18)). M_2 therefore defines the total number of loading cycles considered in the optimisation.

$$F_2(x) = \sum_{i=1}^{M_2} \left(\frac{\Delta \sigma(x)_i^{pre}}{2} - \frac{\Delta \sigma_i^{exp}}{2} \right)^2 \tag{18}$$

Finally, the stress relaxation (or strain hold) loading region is of interest as it represents a period of creep dominant behaviour in the model. Fitting in this region aids in the determination of the viscous stress material constants (Z and n). Stress values predicted in this section ($\sigma(x)_{RELAX\ i}^{pre}$) are compared to experimental values ($\sigma_{RELAX\ i}^{exp}$) in an additional objective function (eq. (19)). M_3 defines the number of relaxation data points considered in the optimisation.

$$F_3(x) = \sum_{i=1}^{M_3} \left(\sigma(x)_{RELAX\ i}^{pre} - \sigma_{RELAX\ i}^{exp} \right)^2 \tag{19}$$

Note that the relaxation objective function (eq. (19)) is of course omitted in optimisation procedures performed on saw tooth strain profile experimental data. Optimisation programs that consider saw tooth experimental data are therefore deemed two objective function procedures. Programs that take into account relaxation data are deemed three objective function procedures. The above objective functions are implemented in an optimisation procedure using MATLAB. The Chaboche differential equations are evaluated using ODE45[17], with gradient method based least squares optimisation[18] completed using the MATLAB function LSQNONLIN[19].

The application of LSQNONLIN through MATLAB in the present work enforces the use of the Levenburg-Marquardt algorithm[20,21]. This is in effect a combination of the steepest decent gradient method and the well known Gauss-Newton method[22]. This approach has been used extensively for the determination of material parameters[4–7], however it is not the only option available to a potential user. For example, material parameters have been optimised using genetic or evolutionary algorithms by Li et. al.[23] and Lin and Yang[24]. Here, initially randomly generated individuals (sets of material constants) are ranked against one another based on some fitness criterion (objective functions). The fittest individuals will survive a generation and are thus allowed to mutate and reproduce, forming a subsequent population of individuals. These algorithms can run for a determined number of generations or until some fitness or mutation limit is satisfied. Alternatively, Egan et. al.[25] have shown that pattern search methods may also be implemented in the determination of material parameters. Small aberrations in parameter values are made in the various free dimensions. An iterative step is then taken in the direction that yields the lowest objective function. Note this is different to gradient methods as a Jacobian is not evaluated. The least squares method of evolution may also be substituted for alternatives, such as the least absolute remainder or one step Sine estimator methods[26]. It is worth pointing out that, regardless of the optimisation routine implemented by a user, the strategies discussed in section 4 can still be applied to accommodate the use of multiple sources of experimental data.

4 Multiple Data Source Optimisation Strategies

4.1 Requirement

Preliminary studies and previous experience has highlighted that, for experiments performed using the same material being loaded under comparable strain ranges and rates (i.e. in situations where a single set of material constants should be sufficient to describe all the test results), different sets of optimised material constants can be derived from each of the experimental data sets. For the implementation of material models like the Chaboche model in component analysis, it is vital that a single set of material constants (i.e. one that is not dependent of experimental loading conditions) that is representative of the material behaviour is derived. A general optimisation procedure has been developed to fine tune material constants[5,6]. It is the intention of this paper to further explore the application of optimisation for the case where two different sets of test data that should be described by the same set of material constants are available. Cao and Lin suggested that the ideal optimisation procedure, when applied to multiple data curves, should give equal opportunity for all experimental curves to be optimised against[27]. With this in mind, the proposed optimisation strategies presented here involve some form of information exchange between sub-optimisation procedures. In this way, material constants are optimised based on all available experimental data.

The inclusion of multiple sets of experimental data offers several possibilities regarding the determination of initial conditions. Hardening material constants can be determined accurately using either saw tooth or relaxation experimental data. Due to the reduced complexity in saw tooth tests (arising due to hardening mechanisms, as opposed to creep, being nearly constantly dominant throughout), these tests are more readily applicable to the initial material constant determination procedure[4,6]. Similarly, creep constants may be estimated from the stress relaxation periods in the relaxation tests, where creep is considered to be dominant in the strain hold region (at least, when the testing temperature is sufficiently high enough to initiate creep). The rate at which a material softens in the linear secondary

region has been found to be consistent for both experimental test types; therefore H (see eq. (6)) can be reasonably estimated from either set.

4.2 Methodologies

4.2.1 Separated Parallel Optimisation (SP)

Given that hardening material constants could be accurately derived from either data set but creep constants may only be realistically determined from relaxation data, a method that would require only a single experimental set to be optimised against would be of great interest. Potentially, only the tests with stress relaxation periods would need to be performed, thus streamlining test programs and reducing the time expended for optimisation. To highlight this effect, separated optimisation methodologies that use different initial conditions have been performed simultaneously (see fig. 5) for different sets of experimental data. These separated procedures entail performing a 2 objective function optimisation process on saw tooth experimental data and a 3 objective function process on the relaxation experimental data. There is no exchange of information between the two objective functions. A summary of the type of experimental data used for the formulation of these objective functions for each experimental data type is presented in fig. 6.
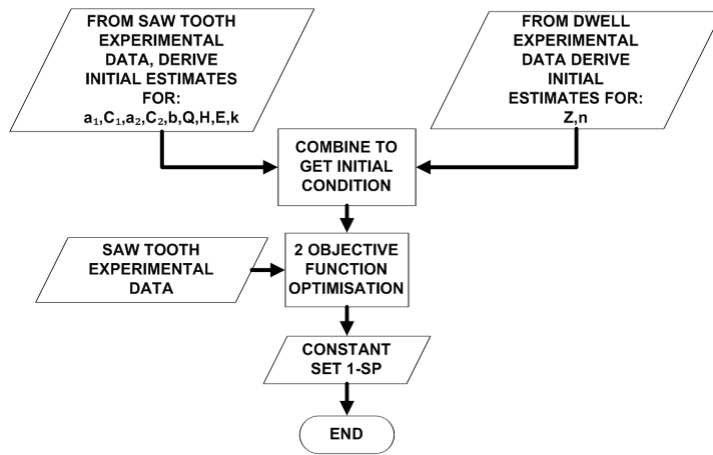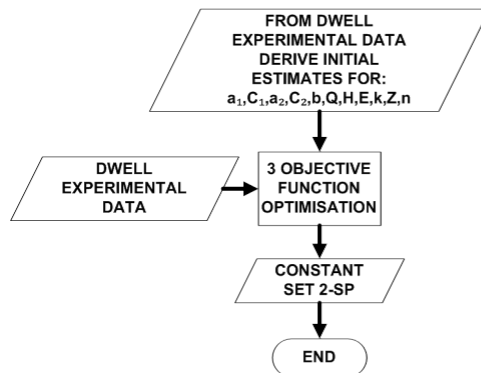
Figure 5: *Flowchart of the separate parallel optimisation procedure, compromising of (a) a two objective function optimisation procedure using Saw Tooth experimental data and (b) a three objective function optimisation procedure using Relaxation experimental data.*
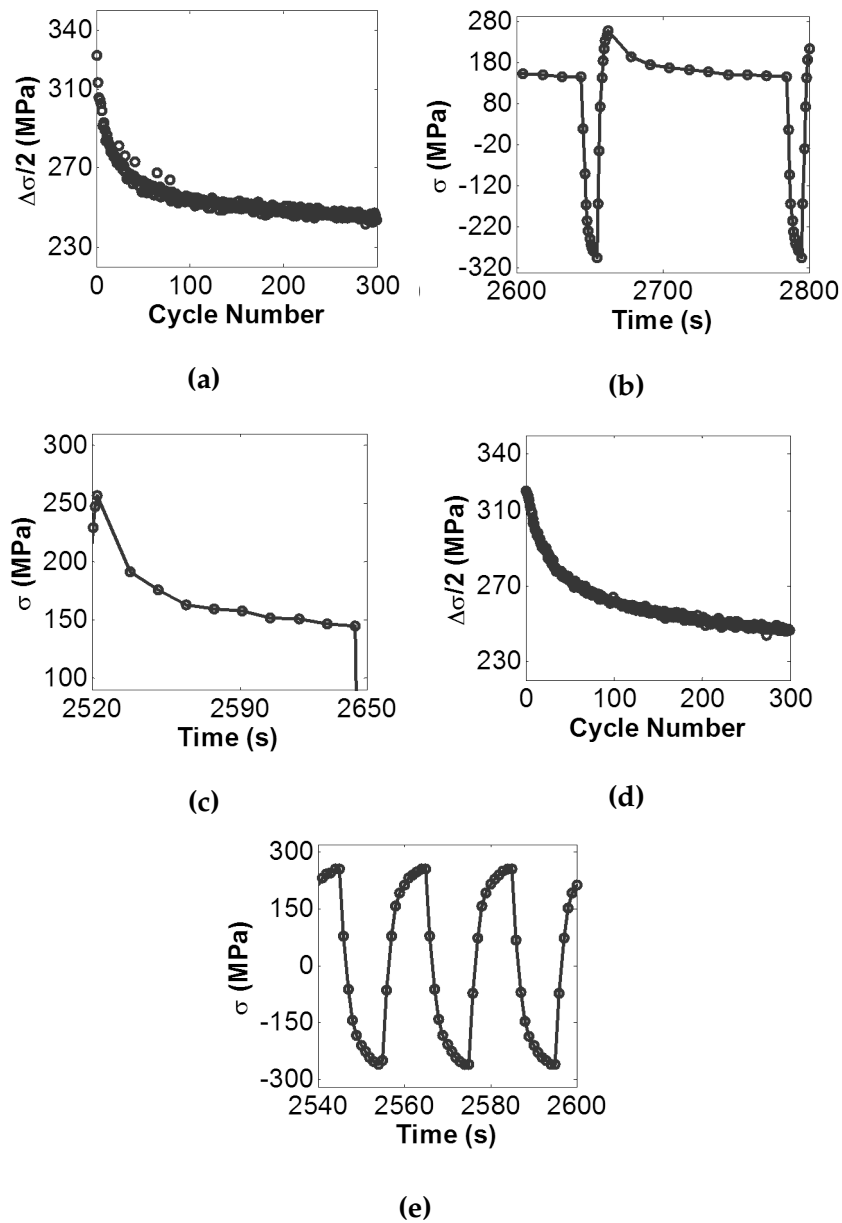
17

Figure 6: *Examples of experimental data used to formulate objective functions for (a) stress range fitting in Relaxation experimental data (b) general stress fitting in Relaxation experimental data (c) stress relaxation region fitting in Relaxation data (d) stress range fitting in Saw Tooth experimental data and (e) general stress fitting in Saw Tooth experimental data.*

4.2.2 Series Optimisation (S)

In the series optimisation methodology (fig. 7), initial material constant estimates are determined from the relevant sections in each experimental data set, as described previously (i.e. hardening material constants from saw tooth experimental data and creep constants from relaxation data). An optimisation procedure is performed using the saw tooth experimental data with a view to "fine tuning" hardening constants. A subsequent optimisation procedure using the first optimised material constant set as an initial condition (constant set 1-S is equal to the initial conditions for the 3 objective function optimisation process in fig. 7) and the relaxation experimental data is completed with a view to determining creep constant values. It is suspected that the change in the hardening constants will be minimal between the constant set 1-S and constant set 2-S (see fig. 7). Both optimised material constant sets have been evaluated and compared to both experiment data types to explore fitting quality. Note constant set 1-S is equal to constant set 1-SP in fig. 5; however constant set 2-S is not necessarily equal to constant set 2-SP due to the different initial conditions used for the same (3 objective function) optimisation procedure.
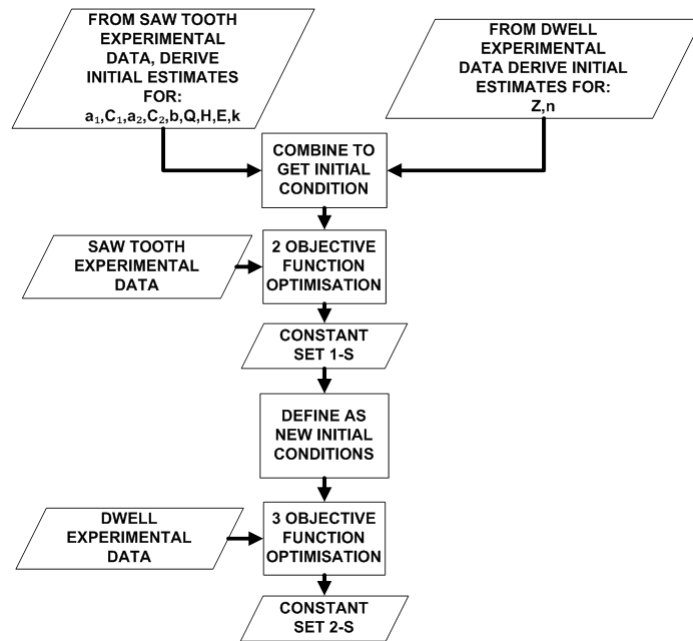
Figure 7: *Flowchart of the series optimisation procedure.*

4.2.3 Combined Parallel Optimisation (CP)

As an alternative to the above two methods (where each experimental data source is considered independently), it is conceivable that a single optimisation procedure could be performed that accounts for both experiment data, thus conducting combined parallel optimisation (see fig. 8). Given some initial conditions (that may be derived in the most efficient way depending on the available data) a total of five objective functions could be derived that effectively combine the two and three objective function optimisation procedures in figs. 5 and 7. Potentially, a single set of material parameters could be derived that would accurately represent both saw tooth and relaxation experimental data. Initial conditions could be derived from either saw tooth or relaxation type experimental data for this optimisation strategy. In the present work, both initial conditions are considered in the results section in order to determine the preferential option.
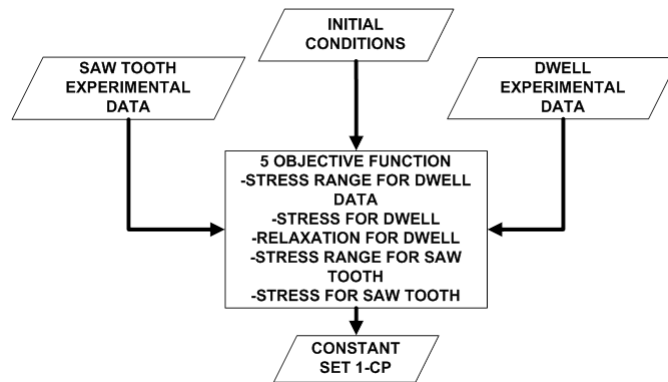
20

Figure 8: *Flowchart of the combined parallel optimisation procedure (see fig. 6 for objective function descriptions).*

5 Results

5.1 Experimental data for a P91 steel at 600°C

Experimental data was generated using an Instron 8862 thermo-mechanical fatigue (TMF) machine. Temperature control is achieved by radio-frequency (RF) induction. Strain limits were set to 0.5%, with a 2 minute hold period at the end of each of the tensile loading regions (where applicable) and a constant strain rate of 0.1%/s. A temperature uniformity requirement in the specimen gauge section was enforced, such that the entire gauge section was within ± 10°Cof the required testing temperature. Typical temperature variations in the gauge section during the test periods were within ± 1°C. Thermocouples were placed along the gauge section, allowing for the monitoring of the axial and circumferential temperature gradients during the design of the induction coil and the calibration procedure. Cyclic testing has been performed on a P91 steel (typically used for high temperature piping components in the power industry) under isothermal conditions (600°C), using saw tooth and relaxation controlling strain profiles. During the experiments, data values (stress, strain and time) were recorded approximately 4 times every second (giving on average 1210 data points per loading cycle for dwell type data). Cyclic softening behaviour (represented by a reduction in stress range with increased accumulated plastic strain) was observed in both test types, as shown in fig. 9[8,28]. The stress versus strain behaviour of P91 at 600°Ccan be seen in fig. 10 for the monotonic loading region and the first full loading cycle of a dwell type load profile. Results for the same material loaded by an identical loading profile can also be seen in fig. 10 for two alternative temperatures (400°Cand 500°C). The chemical composition (by percentage weight) and basic tensile material properties (Youngs modulus, E, yield stress, σ_y, ultimate tensile strength, σ_{UTS}, and the percentage reduction in cross section area at failure) for P91 are given in tables 1 and 2, respectively.

Two sets of initial conditions were derived for the optimisation procedures. Saw tooth and relaxation experimental data were used to find hardening and creep material constants, respectively (deemed "Saw Tooth"

initial conditions, see table 3). Alternatively, a full set of initial conditions were determined solely from relaxation tests ("Relaxation" initial conditions, see table 3). In all optimisation routines the first 300 loading cycles from the experimental data sets were taken into account. Due to the large amount of data generated in testing, the optimisation methodologies are based on a reduced number of data points. 10 experimental data points were selected for each loading region (tensile, compressive or strain hold), giving 20 and 30 data points per loading cycle for saw tooth and dwell type data, respectively.

Table 1: *Chemical composition (wt %) of P91 steel.*

Cr	Mo	Mn	Si	Ni	V	C	Cu
8.49	0.978	0.43	0.37	0.32	0.2	0.11	0.07
Nb	Co	P	W	S	Ti	Al	Fe
0.06	0.02	0.014	< 0.02	0.008	< 0.002	< 0.001	Balance

Table 2: *Basic tensile properties of P91 steel at 600°C.*

$E(GPa)$	$\sigma_y(MPa)$	$\sigma_{UTS}(MPa)$	% Reduction in Area
134	116	315	95.6

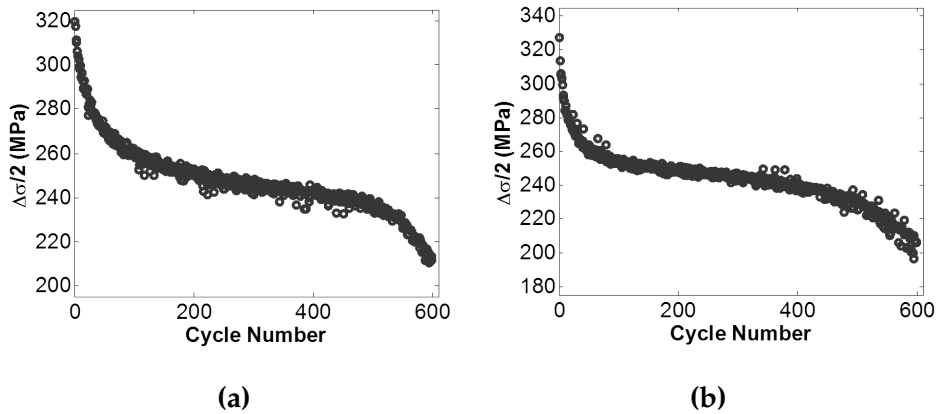**(a)**   **(b)**

Figure 9: *Stress range evolution with cycle number for a P91 steel at 600°C for 600 loading cycles using (a) a saw tooth loading profile and (b) a relaxation loading profile. Note the clear primary, secondary and tertiary regions.*
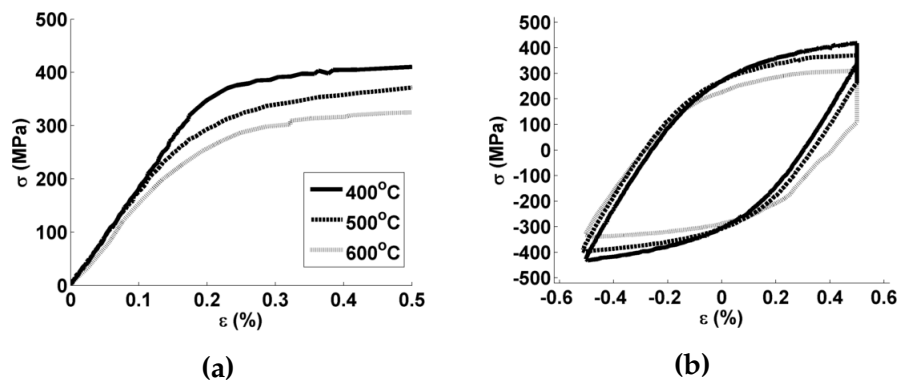
Figure 10: *Isothermal stress versus strain plots showing (a) monotonic loading and (b) first cyclic hysteresis loop for P91 steel at three temperatures (400°C, 500°Cand 600°C). Results are taken from dwell type loading profile data.*

5.2 Optimisation Results

In the separated parallel optimisation procedure, optimisation programs based on the formulation of 2 or 3 objective functions are performed on the relevant experimental data sets. The 2 objective function optimisation is equivalent to the first step in the series optimisation methodology shown in section 4.2.1, therefore the results (constant set 1-S) are identical and are shown in table 3 as constant set 1-SP. Results of the 3 objective function optimisation (constant set 2-SP) are also presented in table 33.

Using series optimisation, hardening material constants are fine-tuned from the initial conditions derived from both saw tooth and relaxation experimental data using a 2 objective function optimisation procedure (considering the fitting to saw tooth data only). This gives rise to constant set 1-S (equivalent to 1-SP in table 3), which is used as an initial condition in the 3 objective function optimisation that fine tunes creep material constants, incorporating relaxation experimental data (constant set 2-S, see table 3 for results). Hardening material constants should be common for both data sets as creep is a dominant mechanism only in the stress relaxation loading regions, therefore it is to be expected that constant set 2-S should represent both sets of experimental data well.

In combined parallel optimisation, a single procedure is undertaken that evaluates 5 objective functions, calling both sets of experimental data for comparison. Initial conditions could be determined using both saw tooth and relaxation data or just relaxation data. Additionally, an averaged initial condition set (based on the two initial condition sets) can be applied (see table 3).

Table 3: *Summary of initial estimates and optimised values for the Chaboche model material constants using different optimisation procedures.*

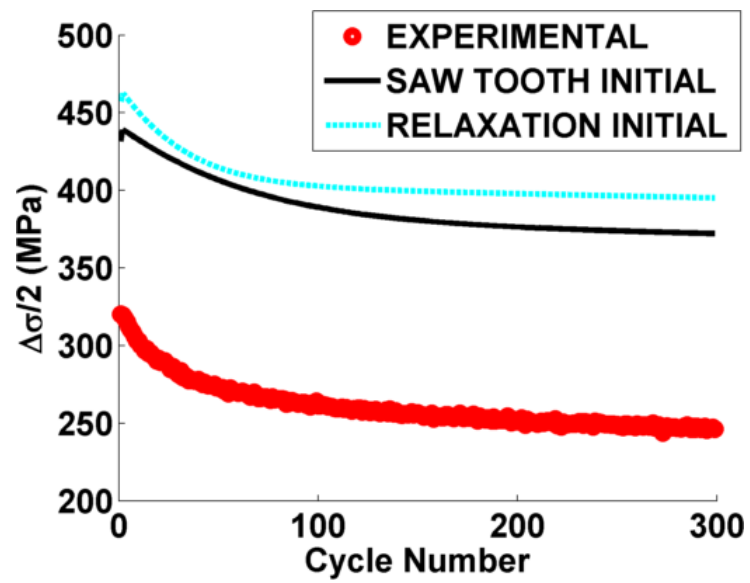|	Saw tooth initial constants	Relaxation initial constants	Constant set 1-SP (equal to Constant set 1-S)	Constant set 2-SP	Constant set 2-S	Constant set 1-CP from Saw tooth initial conditions	Constant set 1-CP from Relaxation initial conditions
a_1 (MPa)	85.18	92.91	2.81	66.90	18.06	80.96	86.75
C_1	1360.66	1164.23	2132.51	2516.18	538.24	1572.18	1422.08
a_2 (MPa)	95.81	104.03	62.19	88.93	50.79	90.69	59.85
C_2	551.75	433.47	644.01	506.55	586.93	519.50	671.78
Z $(MPa.s^{1/n})$	752.99	752.99	1259.01	683.03	1004.19	697.45	674.11
n	6.87	6.87	4.11	5.01	3.16	5.44	5.00
b	1.86	3.67	5.41	1.18	34.65	4.64	2.92
Q (MPa)	-70.64	-74.56	-38.49	-84.06	-71.85	-77.78	-84.14
k (MPa)	9.39	33.33	0.51	30.90	143.90	146.04	30.66
E (GPa)	140.34	148.09	140.82	153.66	140.90	146.04	153.85
H	-2.99	-3.16	-3.74	-2.83	-1.98	-3.06	-2.82

6 Comparative Plots

6.1 Saw Tooth waveform prediction

In order to assess the predictive capability of the Chaboche model using optimised material constant sets, "plotting" programs were implemented. Strain limits and rates from experimental data were used to define a loading profile with uniform time and strain increments. The Chaboche model is used to calculate the evolution of the state variables using this uniform profile; hence noise and scatter that are apparent in the experimental data are not reproduced, making study of the resultant curves easier. Comparison between this predictive curve and the original experimental data is still valid as both are dependent on loading profiles generated using the same characteristic parameters (such as strain limits values or strain rate). Through comparison of predicted and experimental data, the coefficient of determination (r^2) may be calculated for each optimised material constant set (see table 4). These values provide a metric by which to judge the fitting quality of a predictive model (comparing to experimental data)[22]. Coefficients of determination are calucalted from eq. (20) for N data points, where EXP_i and $PRED_i$ are the ith experimental and predicted values, respectively, and σ_{EXP} is the standard deviation of the experimental data. A perfect fitting (i.e. with no error between experimental and fitted data points) would result in an r^2 value of 1. Note that, in the present work, all available experimental data was used to determined r^2 values (this differs from the optimisation process, where only a selected number of experimental points were implemented in order to keep computation times reasonable). Plots comparing specific predicted loading cycles to the corresponding experimental data are presented for stress range prediction and general cyclic stress fitting for the middle (150th) cycles. For clarity, the profiles predicted by each constant set are separated into multiple plots. Those predicted from initial conditions may be found in fig. 11. Profiles predicted from the results of separated parallel or series optimisation can be seen in fig. 12. Profiles predicted using the results of combined parallel optimisation are given in fig. 13.
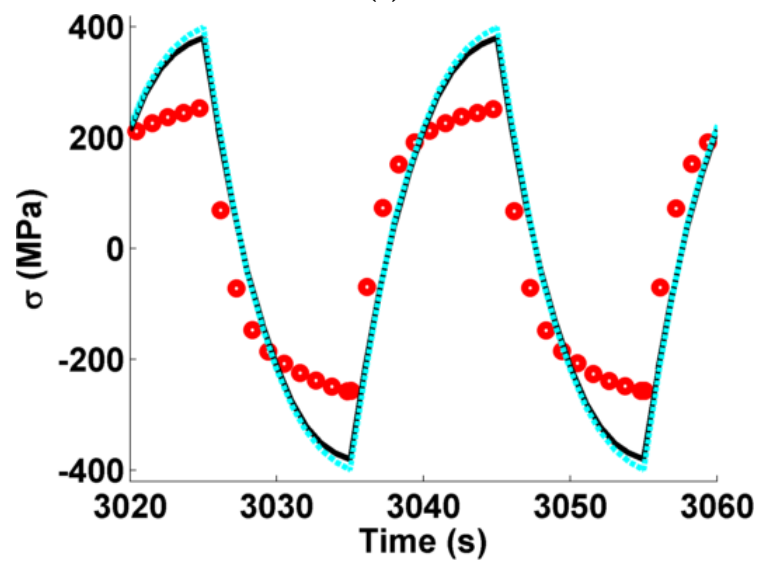
$$r^2 = 1 - \sum_{i=1}^{N} \frac{(EXP_i - PRED_i)^2}{N\sigma_{EXP}^2} \qquad (20)$$

Table 4: *Summary of coefficients of determination for fitting to saw tooth experimental data using different material constant sets.*

|	r^2
Saw tooth initial conditions	0.7630
Relaxation initial conditions	0.7215
1-SP (equal to 1-S)	0.9977
2-SP	0.9907
2-S	0.9958
1-CP - Saw tooth initial conditions	0.9765
1-CP - Relaxation initial conditions	0.9988

(a)

(b)

Figure 11: *Illustration of fitting quality for saw tooth loading profile using initial estimates of the material constants, showing (a) stress range evolution with cycle number, (b) stress fitting for the middle (150th) cycles.*
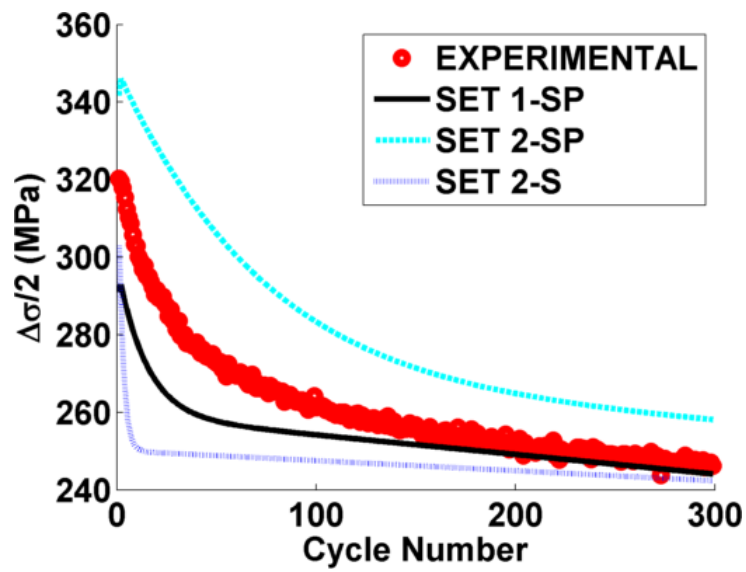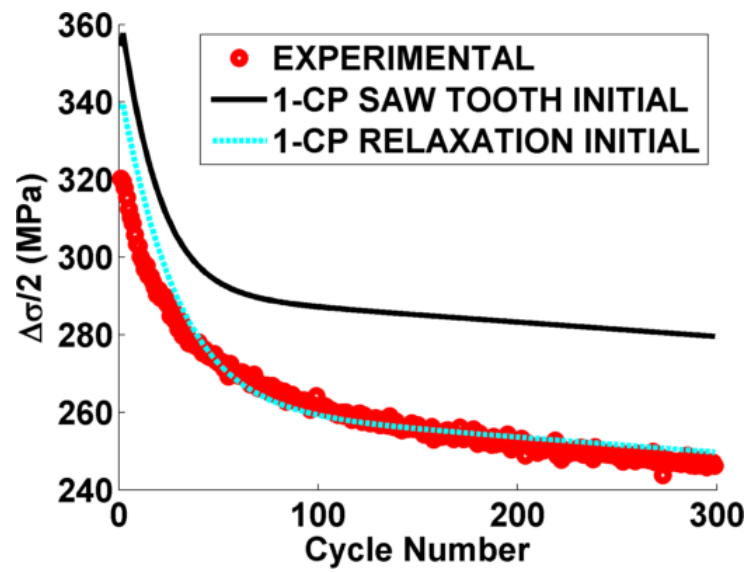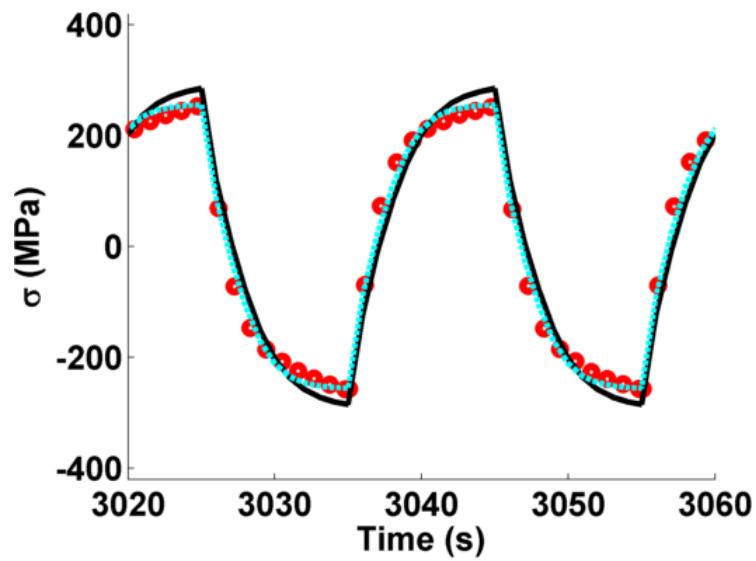
(a)
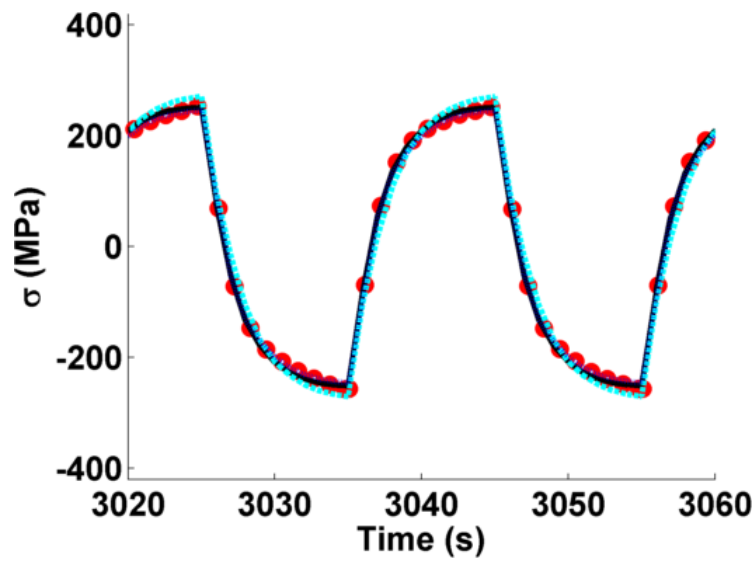
(b)

Figure 12: *Illustration of fitting quality for saw tooth loading profile using optimised values of the material constants from series and illustration of fitting quality for saw tooth loading profile using optimised values of the material constants from separate parallel optimisation procedures. Plots shown are (a) stress range evolution with cycle number, (b) stress fitting for the middle (150th) cycles.*
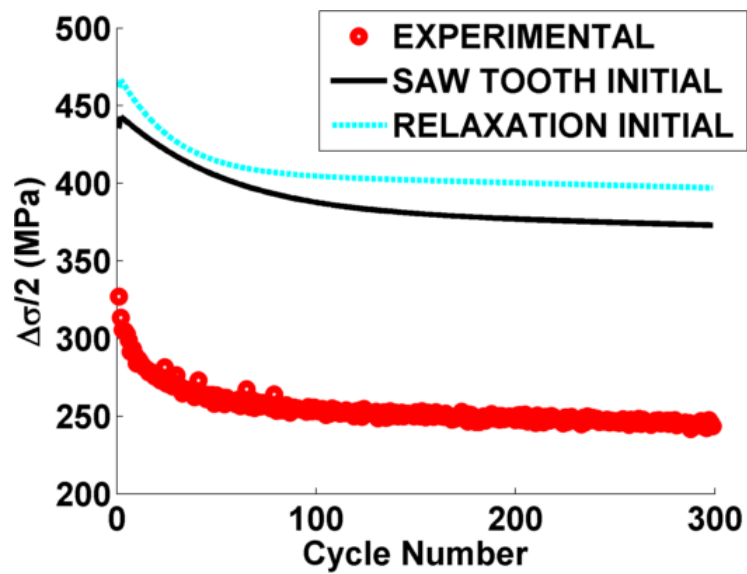
(a)

(b)

Figure 13: *Illustration of fitting quality for saw tooth loading profile using optimised values of the material constants from combined parallel optimisation procedures, showing (a) stress range evolution with cycle number, (b) stress fitting for the middle (150th) cycles.*

6.2 Relaxation waveform prediction

Similarly to section 6.1, coefficient of determination (r^2) values are presented for each material constant set based on relaxation experimental data (see table 5). To demonstrate the relative fitting of the predicted profiles (based on different material constant sets), graphical representations comparing specific predicted profiles to experimental data are presented for stress range prediction and general cyclic stress fitting for the middle (150th) cycles are also presented. For clarity, the predicted profiles are also separated into initial conditions, series and separated parallel optimisation results and combined parallel optimisation results groups (see figs. 14 to 16, respectively).

Table 5: *Summary of coefficients of determination for fitting to relaxation experimental data using different material constant sets.*

|	r^2
Saw tooth initial conditions	0.7599
Relaxation initial conditions	0.6909
1-SP (equal to 1-S)	0.9310
2-SP	0.9853
2-S	0.9947
1-CP - Saw tooth initial conditions	0.9786
1-CP - Relaxation initial conditions	0.9994
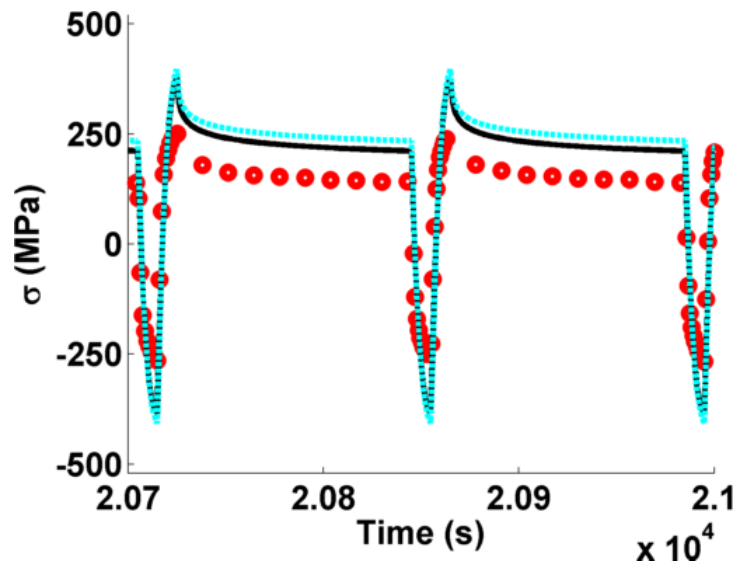
Figure 14: *Illustration of fitting quality for relaxation loading profile using initial estimates of the material constants, showing (a) stress range evolution with cycle number, (b) stress fitting for the middle (150th) cycles.*
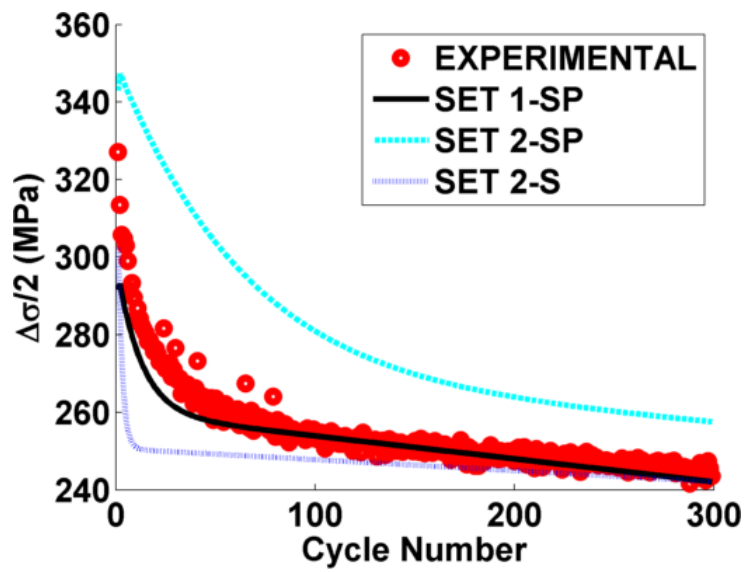
(a)
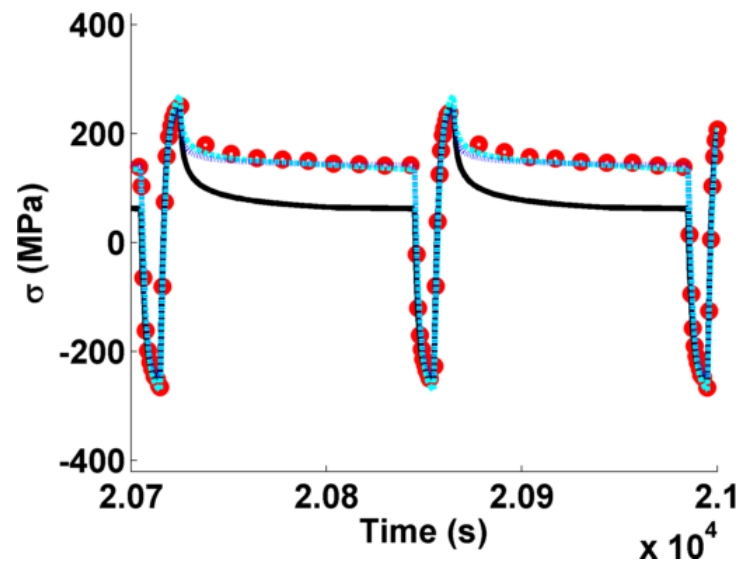
(b)

Figure 15: *Illustration of fitting quality for relaxation loading profile using optimised values of the material constants from series and illustration of fitting quality for relaxation loading profile using optimised values of the material constants from separate parallel optimisation procedures. Plots show (a) stress range evolution with cycle number, (b) stress fitting for the middle (150th) cycles.*

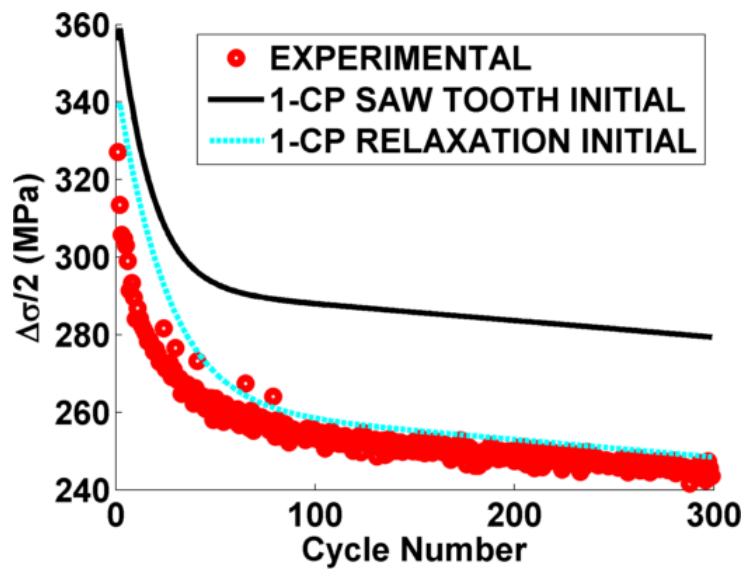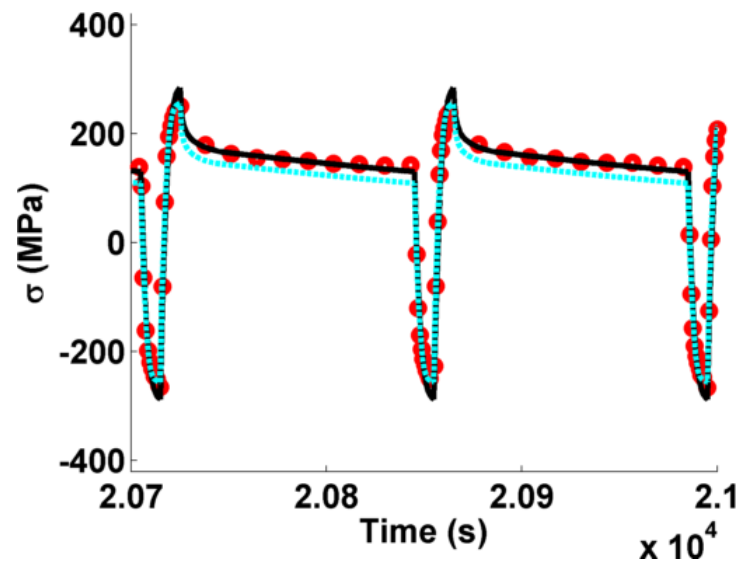**(a)**

(b)

Figure 16: *Illustration of fitting quality for relaxation loading profile using optimised values of the material constants from combined parallel optimisation procedures, showing (a) stress range evolution with cycle number, (b) stress fitting for the middle (150th) cycles.*

35

7 Discussion

A single set of material constants for the Chaboche visco-plasticity model should be sufficient to describe multiple sets of experimental data if the tests were performed under the same characteristic conditions (e.g. isothermal tests at the same temperature, similar strain rates and limit strain values). Several optimisation strategies have been presented to meet this expectation. While the resultant material constant sets from the optimisation procedures differ considerably, the general fitting quality was greatly improved and was generally consistent (see tables 4 and 5) through optimisation (highlighting the complex interplay between material constants in the Chaboche model). The first step in the practical application of a model is to determine a single, representative set of material constants[7].

Optimisation procedures using the separated parallel strategy ran simultaneously (but with no exchange of information between the two procedures). While constant set 1-SP is slightly better (r^2 equal to 0.9977 compared to 0.9901 for constant set 2-SP) at predicting saw tooth experimental data, constant set 2-SP is significantly more adept at predicting relaxation experimental data (r^2 equal to 0.9853 compared to 0.9310 for constant set 1-SP, see table 5). Such behaviour is to be expected as constant set 1-SP is not the result of an optimisation based on experimental data containing stress relaxation regions, therefore creep material constants cannot be fitted to a creep dominant region. The separated nature of this methodology means that inevitably one of the optimised material constant sets is redundant; therefore the experimental data related to this redundant material constant set is not represented in the final solution. If multiple experimental data sets are available, the maximum confidence in the final solutions ability to predict experimental data can be obtained by applying to highest level of constraint to an optimisation procedure.

The series optimisation strategy (fig. 7) effectively dissects sources of experimental data on a mechanism basis. Completion times for this optimisation methodology have been found to be relatively lengthy (approximately 8 hours compared to 5 hours for the separate parallel optimisation procedures). More importantly however, the subsequent consideration of

relaxation data after the saw tooth optimisation procedure could detract from the ability of the final result to predict the saw tooth experimental response. Given slight experimental discrepancies between the hardening sections in both experimental data sets, it is reasonable to assume that different optimum hardening material constants (i.e. a_1, C_1, a_2, C_2, b and Q) will better predict these marginally different stress profiles. As the relaxation experimental data is considered last, its hardening loops are treated preferentially, altering the material constant values that predict the saw tooth data well in order to predict the relaxation data. The fitting quality to saw tooth experimental data is thus compromised. Such behaviour can be observed in table 4, noting that the coefficient of determination value reduces marginally between constant set 1-S (0.9977) and 2-S (0.9958). When predicting relaxation data, the additional optimisation procedure improves the fitting quality (the coefficient of determination value is greater for constant set 2-S than 1-S see table 5). In order to give adequate and equal consideration to both sources of experimental data, simultaneous (or parallel) optimisation has been performed.

In the combined parallel optimisation strategy (fig. 8), objective functions are formed using both sets of experimental data simultaneously. Completion times are generally significantly less for the combined parallel optimisation methodology (approximately 3 hours) than for the alternatives suggested. It is suspected that this is due to the high level of constraint in this methodology. The formation of the objective function is dependent on several sub-objective functions, therefore the gradient based optimisation method used in LSQNONLIN[19] has more information to determine the direction of greatest decent. Minimum (either global or local) solutions can therefore be obtained in a shorter time.

Initial estimates derived from either set of experimental data generally predict the same hardening behaviour (see fig. 11); despite slight differences in the related material constant values. Although the creep constants Z and n are identical for the two initial condition sets (having both been derived from relaxation data), a small discrepancy can be observed between the stress relaxation curves prediction by the saw tooth initial condition set and the relaxation initial condition set in fig. 14. It should be remembered

37

that the stress relaxation region in the relaxation experimental data does not represent a period of solely creep dependant behaviour. Isolation of material constants based on controlling deformation mechanisms has not been possible in the present work and should only be undertaken with extreme care.

All optimised material constant sets appear to predict saw tooth experimental data well (see figs. 12 and 13 and table 4). Constant set 1-SP (or 1-S) appears to give the optimum solution for the prediction the results of saw tooth experiments (see table 4). This is to be expected as the constant set is determined based solely on objective functions formed from saw tooth experimental data. The lack of additional constrain from other experimental data sources means that the fitting quality of this material constant set is not impaired (when compared to saw tooth experimental data). Note that for constant set 1-CP Relaxation (see table 4), the fitting quality is approximately the same as for constant sets 2-SP and 2-S (approximately 0.99). Lower r^2 values are observed for constant sets 1-CP Saw Tooth. A potential explanation for this phenomenon is that the combination of initial condition values derived from both saw tooth and relaxation experimental data does not represent a unified material constant set. The division of initial condition values based on a mechanism basis does not reflect the interplay between hardening and creep effects present in the Chaboche model. These initial conditions therefore may cause the optimisation to localise on non-optimum solutions, impairing the fitting quality in some cases and resulting in a lower r^2 value.

The comparative plotting results for the prediction of relaxation experimental data are more complex, owing to the rejection of creep dominant regions for the optimisation of some material constant sets (constant set 1-SP). The effects of not optimising using experimental data with creep dominant regions can be illustrated by the relatively poor prediction of stress relaxation using material constant set 1-SP (see fig. 15 and table 5). A marked improvement in creep response prediction can be seen for constant set 2-S (i.e. after constant set 1-S has been optimised based on data with creep dominant regions). Both combined parallel optimisation material constant sets estimate the relaxation experimental data well, however the

inclusion of congruent initial conditions (i.e. derived from one experimental data source; the relaxation experimental data) in determining the constant set 1-CP Relaxation seems to provide a better approximation of the stress range evolution, compared to constant sets 1-CP Saw Tooth and 1-CP Average.

8 Recommendations for Potential Users

The optimisation of multiple material constants based on several experimental data sources is complex and there are many potential difficulties that can arise. To aid any readers who may wish to implement similar optimisation procedures, the following highlights several key problems and the author's suggested solutions.

Optimisation problems can often encounter some form of numerical instability and fail. It is the author's experience that this generally due to initial data identification. Lengthy experiments such as the isothermal cyclic tests presented in fig. 9 will usually generate many data points. It is therefore critical that automated data handling be implemented. This will typically include some form of data selection or filtering (it could be very inefficient to solves ODE's and evaluate objective functions for every data point). Due to experimental scatter, it is possible for small aberrations in, say, stress to occur and thus be passed to the optimisation routine. These small aberrations can prevent ODE solving algorithms completing and thus stop the evaluation of objective functions. It is vital that adequate filters be applied to the initial data interpretation procedure in order to prevent excessive data scatter impeding ODE algorithms. In the present work, experiential data was cleaned prior to optimisation[29].

Optimisation procedures may also result in the determination of physically unrealistic constants. Alternatively, a dependence may be observed between an particular optimisation method and the solution. It should be noted that, particularly in the case of the Chaboche model presented here, the highly multi-dimensional (i.e. numerous parameters to be optimised) nature of the optimisation creates a complex topology. This is exacerbated by the potential for strong dependencies between material constants. It is therefore possible for gradient methods to converge on drastically different minima with only slight difference in initial estimate. This point is particularly true in the context of the present work, where prior optimisation procedures yield the initial estimates for subsequent optimisations (see fig. 7 for example). Solutions can be made more reliable by using side constraints in the optimisation. Isotropic parameters in eq. (6) such as Q

and H can typically be determined with a great deal of certainty. Tight upper and lower limits can therefore be applied to these constants, while allowing the other material constants to be fully optimised. Applying tight side constraints must be done with caution due to potential parameter interactions. Additionally, the maximum level of constraint should be enforced from experimental data. It is the conclusion of this work that all available experimental data (even when it is from different sources/tests) should be used to evaluate objective functions in the same optimisation iteration.

9 Conclusions and Future Work

- It is vital for practical implementation of material models, that a single set of material constant values can be determined from comparable laboratory tests. When comparing experimental results however, the effects of material property scatter and experiment repeatability must be also taken into account as a possible explanation for minor discrepancies.

- After the determination of a representative material constant set, a practical components response due to, say, cyclic loading could be estimated. In this work, the Chaboche model has been applied due to the high importance placed on optimisation in material parameter determination procedures[5,6].

- If multiple experimental data sources are available that should be described by the same material constant set, objective functions in optimisation procedures should be evaluated simultaneously (i.e. in the same optimisation iteration) based on all available experimental data sources (combined parallel optimisation). This procedure enforces the maximum level of constraint on the optimisation procedure and does not lead to preferential fitting of one data source over another. Combined parallel optimisation procedures generally give rise to higher coefficients of determination (indicating superior fitting) and have shorter computation times.

- Successive optimisation methodologies, whereby each experimental data source is considered in turn, tends to lead to a preferential fitting to the experimental data source considered last.

- Relaxation type cyclic tests (where strain hold periods are introduced) are preferable for material constant determination in comparison to tests where no stress relaxation takes place due to the dominance of creep in these regions.

- Initial conditions used in optimisation procedures should be congruent (i.e. derived from a single experimental data source) due to the

complex interplay between creep and hardening mechanisms in the Chaboche model.

- A single testing condition was considered in the present work. The Chaboche model implemented does not include strain rate, strain range or temperature effects, therefore the material constants derived cannot be applied to other testing conditions (although limited extrapolation may be possible in a range that does not change the controlling deformation mechanism). Some success has been achieved in the past by interpolating material constant values for different loading conditions (e.g. temperature); however future work will look to expand the applicability of the Chaboche model. The optimisation procedure detailed in the present work can then be implemented with confidence in order to determine related material constants, allowing for more complex component analyses (such as full thermo-mechanical fatigue) to be conducted.

- Future work will attempt to verify the response predicted by material constants (optimised from uniform experimental data) for typical non-uniform component loading cycles.

- Temperature, strain rate and strain limit dependencies will also be investigated in order to establish TMF (thermo-mechanical fatigue) life estimation procedures. Improved long term creep response may also be examined through some form of dynamic recovery term, similar to those suggested by Tong and Vermeulen[2] and Zhan and Tong[4,30].

10   Acknowledgements

References

[1] Chaboche JL. Time-independent constitutive theories for cyclic plasticity. International Journal of Plasticity. 1986;2(2):149 – 188.

[2] Tong J, Vermeulen B. The description of cyclic plasticity and viscoplasticity of waspaloy using unified constitutive equations. International Journal of Fatigue. 2003;25(5):413 – 420.

[3] Tong J, Zhan ZL, Vermeulen B. Modelling of cyclic plasticity and viscoplasticity of a nickel-based alloy using Chaboche constitutive equations. International Journal of Fatigue. 2004;26(8):829 – 837.

[4] Zhan ZL, Tong J. A study of cyclic plasticity and viscoplasticity in a new nickel-based superalloy using unified constitutive equations. Part I: Evaluation and determination of material parameters. Mechanics of Materials. 2007;39(1):64–72.

[5] Gong YP, Hyde CJ, Sun W, Hyde TH. Determination of material properties in the Chaboche unified viscoplasticity model. Proceedings of the Institution of Mechanical Engineers Part L-Journal of Materials - Design and Applications. 2010;224(L1):19–29.

[6] Hyde CJ, Sun W, Leen SB. Cyclic thermo-mechanical material modelling and testing of 316 stainless steel. International Journal of Pressure Vessels and Piping. 2010;87(6, SI):365–372.

[7] Hyde TH, Sun W, Tang A. Determination of material constants in creep continuum damage constitutive equations. Strain. 1998 AUG;34(3):83–90.

[8] Dowling NE. Mechanical behavior of materials: engineering methods for deformation, fracture, and fatigue. Pearson/Prentice Hall Upper Sadle River, NJ; 2007.

[9] Chaboche J J, Rosselier G. On the Plastic and Viscoplastic Constitutive-Equations .1. Rules Developed with Internal Variable Concept [Art-

icle]. Journal of Pressure Vessel Technology-Transactions of the ASME. 1983;105(2):153–158.

[10] Chaboche J J, Rosselier G. On the Plastic and Viscoplastic Constitutive-Equations .2. Application of Internal Variable Concepts to the 316 Stainless-Steel. Journal of Pressure Vessel Technology-Transactions of the ASME. 1983;105(2):159–164.

[11] Lemaitre J, Chaboche JL. Mechanics of solid materials. Cambridge university press; 1994.

[12] Dieter GE, Bacon D. Mechanical metallurgy. vol. 3. McGraw-Hill New York; 1986.

[13] Mroz Z. On the description of anisotropic workhardening. Journal of the Mechanics and Physics of Solids. 1967;15(3):163 – 175.

[14] Prager W. The Theory of Plasticity: A Survey of Recent Achievements. Proceedings of the Institution of Mechanical Engineers. 1955;169(1):41–57.

[15] Ziegler H. A modification of Prager's hardening rule. Quarterly of Applied Mathematics. 1959;17:55 – 65.

[16] Dafalias YF, Popov EP. Plastic Internal Variables Formalism of Cyclic Plasticity. Journal of Applied Mechanics. 1976;43(4):645 – 651.

[17] T M, Inc. MATLAB 7 User Manual; 2008.

[18] Hooke R, Jeeves T. Direct Search Solution of Numerical and Statistical Problems. Journal of the ACM. 1961;8(2):212–229.

[19] T M, Inc. Optimisation Toolbox 4 User's Guide; 2008.

[20] Levenberg K. A Method for the Solution of Certain Non-Linear Problems in Least Squares. Quarterly of Applied Mathematics. 1944;2(2):164 – 168.

[21] Marquardt DW. An Algorithm for the Least-Squares Estimation of Non-Linear Parameters. SIAM Journal of Applied Mathematics. 1963;11(2):431 – 441.

[22] Chapra SC, Canale RP. Numerical methods for engineers. vol. 2. McGraw-Hill; 2010.

[23] Li B, Lin J, Yao X. A novel evolutionary algorithm for determining unified creep damage constitutive equations. International Journal of Mechanical Sciences. 2002;44(5):987 – 1002.

[24] Lin J, Yang J. GA-based multiple objective optimisation for determining viscoplastic constitutive equations for superplastic alloys. International Journal of Plasticity. 1999;15(11):1181 – 1196.

[25] Egan P, Whelan MP, Lakestani F, Connelly MJ. Small punch test: An approach to solve the inverse problem by deformation shape and finite element optimization. Computational Materials Science. 2007;40(1):33 – 39.

[26] Hill RW, Holland PW. Two Robust Alternatives to Least-Squares Regression. Journal of the American Statistical Association. 1977;72(360a):828–833.

[27] Cao J, Lin J. A study on formulation of objective functions for determining material models. International Journal of Mechanical Sciences. 2008 FEB;50(2):193–204.

[28] Stephens RI, Fuchs HO. Metal fatigue in engineering. Wiley New York; 2001.

[29] Rouse J, Hyde CJ, Sun W, Hyde TH. A Method for the Effective Determination of Cyclic-Visco-Plasticity Material Properties Using an Optimisation Procedure and Experimental Data Exhibiting Scatter. Materials at High Temperatures. Accepted;.

[30] Zhan ZL, Tong J. A study of cyclic plasticity and viscoplasticity in a new nickel-based superalloy using unified constitutive equations.

Part II: Simulation of cyclic stress relaxation. Mechanics of Materials. 2007;39(1):73–80.